Semiconductor Physics, Quantum Electronics & Optoelectronics. 2002. V. 5, N 3. P. 284-287.

PACS: 42.40.Eq, 78.30.Ly

Study of non-reversible photostructural transformations in $As_{40}S_{60-x}Se_x$ layers applied for fabrication of holographic protective elements

A.V. Stronski[1], M.Vlcek[2], S.A. Kostyukevych[3], V.M. Tomchuk[3], E.V. Kostyukevych[3], S.V. Svechnikov[3], A.A. Kudryavtsev[3], N.L. Moskalenko[3], A.A. Koptyukh[3]

[1)] *Polight Technologies Ltd., 291 Cambridge Science Park, Cambridge, CB OWF, UK*
[2)] *University of Pardubice, Pardubice, 53210, Czech Republic*
[3)] *Institute of Semiconductor Physics, NAS of Ukraine, 41 prospect Nauky, 03028 Kyiv, Ukraine*

Abstract. Thin vacuum-evaporated layers of $As_{40}S_{60-x}Se_x$ composition are investigated using Raman spectroscopy from the viewpoint of thermo- and photostructural transformations in them. These transformations are considered as changes in their network structure including three types of piramidal units $AsS_{3/2}$, $AsSe_{3/2}$ and $AsS(Se)_{3/2}$ as well as $As_4S(Se)_4$ and $S(Se)_n$ fragments in its initial state. Annealing or light exposure result in polymerization of the molecular groups and the decreasing number of homopolar bonds, which is thermodynamically favorable. Characteristics of sensivity to photon and electron exposure were investigated. Diffraction efficiency perfomances of a microrelief fabricated using these layers are presented.

Keywords: thin chalcogenide layer, non-reversible transformation, photostructural transformation, Raman spectroscopy, holographic protective elements.

Paper received 15.07.02; revised manuscript received 02.09.02; accepted for publication 10.12.02.

1. Introduction

Chalcogenide glasses of As-S-Se compositions are perspective materials for many technological applications: holography, microlithography, information storage, optoelectronics, etc. [1-6]. The application possibilities are connected with their imaging abilities due to various photostructural transformations under the influence of the external factors: UV, VIS light, e-beams, X-rays, etc. These photostructural changes in evaporated films are understood as changes in their network structure. The microscopic network change is accompanied by macroscopic ones – in optical, chemical, mechanical properties. Raman spectroscopy is the useful method for observation of such changes in the microscopic network. It is non-destructive technique, which can bring information on the changes in chemical bonding and molecular structure of chalcogenide vitreous semiconductor (ChVS) films. This paper deals with the photostructural transformations in vacuum-evaporated $As_{40}S_{20}Se_{40}$ layers studied by Raman spectroscopy.

2. Experiment

The bulk $As_{40}S_{20}Se_{40}$ materials were prepared by the direct synthesis from 5 N purity elements in evacuated quartz ampoules at 700–750 °C for 8–24 h. After synthesis, the ampoules were quenched in a water at a temperature of ~15 °C, which is equivalent to a cooling rate of the order of 10 K/s. In some cases $As_{40}S_{20}Se_{40}$ glasses produced by the commercial company (SDB "Quant", Uzhgorod, Ukraine) were used. Thin ChVS films (d = 0.4–5 μm) were deposited by the vacuum thermal evaporation ($p = 10^{-3}$ Pa) from the resistance-heated quartz or Mo boats onto clean glass substrates (microscopic slides) kept under room temperature. Deposition rate was continuously measured using the quartz microbalance technique, and in the present study it was within 1–6.0 nm/s. Exposure was carried out either by halogen lamp (I = = 20 mW/cm^2, IR cut-off filter) or by natural light. Some samples were annealed at $T = T_g - 20$ °C, where T_g stands for glass transition temperature.

The Raman spectroscopy investigations were carried out by using Fourier transformation IR spectrophotometer IFS55 with FRA 106 Raman module, Bruker, Germany). The laser irradiation at the wavelength of 1.06 μm (having an output power 90 mW during measurements of glasses and 15 mW for measurements of the films) was used for the excitation of the Raman spectra. In our case, this wavelength value was essential because irradiation of samples in this range causes no detectable photo-structural transformations within the scale of 100 scans for glasses and 1000 scans for films. The resolution of the Raman spectrometer was 1 cm^{-1}. All the experiments were performed at room temperature. For analy-

© 2002, Institute of Semiconductor Physics, National Academy of Sciences of Ukraine

sis, the Raman spectra have been reduced by the Shuker-Gammon method [7] and normalized by area.

3. Results and discussion

For Raman spectra of $As_{40}S_{60}$ and $As_{40}Se_{60}$ glasses (Fig.1b), the broad bands with maxima at 345 and 232 cm^{-1}, respectively, are dominant features. Usually they are described within the frames of the molecular model [8]. For more detailed analysis of Raman spectra of $As_{40}S_{60}$ ($As_{40}Se_{60}$) glasses it is necessary to take into account main types of its initial structural units: heteropolar As-S (As-Se) bonds in the framework of AsS_3 ($AsSe_3$) pyramids, bridge As-S-As (As-Se-As) complexes, homopolar As-As or S-S (Se-Se) bonds in different, fully or partially polymerized molecular fragments. The dominant feature of the $As_{40}S_{60}$ is the $AsS_{3/2}$ pyramidal unit (strong band at 345 cm^{-1}). Main band is asymmetrical and is the result of overlap of several bands, see for example peculiarities at 316, 363, 381, 400 cm^{-1}. There are also detectable bands from structural units containing homopolar As-As and S-S- bonds (bands at 191, 223, 235 and 495 cm^{-1}). The peak at 363 cm^{-1} is attributed to the presence of As_4S_4 structural units, which contain As-As bonds. The wide shoulder in 380–400 cm^{-1} region is attributed to the interaction between AsS_3 pyramids. Raman spectra of $As_{40}Se_{60}$ glass have the similar structure: the strong band at 232 cm^{-1} (the largest part of structural units are $AsSe_3$ pyramids) with peculiarities at 249 and 281 cm^{-1} and weak 111 and 142 cm^{-1} bands.

It can be expected that for intermediate $As_{40}S_{60-x}Se_x$ compositions the $AsS_{3/2}$ and $AsSe_{3/2}$ pyramidal units will also represent the largest number of structural units. And indeed, spectra of $As_{40}S_{20}Se_{40}$ glasses (Fig.1a, curve 1) show two-phase structure (dominant features are the two main broad bands with maxima at 244 and 355 cm^{-1}). It should be pointed out that both bands are asymmetrical and they are the result of overlapping several bands. Sum of the Raman spectra of $As_{40}S_{60}$ and $As_{40}Se_{60}$ glasses taken with necessary ratio (1/3 and 2/3, respectively) gives good rough approximation for Raman spectra of $As_{40}S_{20}Se_{40}$ glasses (Fig.1a, curve 2). But, as can be seen from the Fig.1a, experimentally obtained Raman spectra of $As_{40}S_{20}Se_{40}$ glasses are somewhat different of that for the curve 2. Difference spectra (Fig.1a, curve 3) show bands with maxima at 257 and 361 cm^{-1}. It is possible to consider this as indication of the increased presence of Se_n chains (band 258 cm^{-1}) and As_4S_4 (363 cm^{-1}) molecular fragments. Also it can be related to the presence of the mixed $AsS(Se)_{3/2}$ pyramidal structural units in addition to $AsS_{3/2}$ and $AsSe_{3/2}$ units in the network of $As_{40}S_{20}Se_{40}$ glass. Frequencies of their vibrational modes are different from that of $AsS_{3/2}$ and $AsSe_{3/2}$ structural units [9].

We can see that the two-phase structure for Raman spectra of as-evaporated $As_{40}S_{20}Se_{40}$ films is preserved as well (Fig.2 curve 1). Raman spectra of as-evaporated $As_{40}S_{20}Se_{40}$ films (Fig.2 curve 1, Fig.3, curve 1) also show the presence of numerous weak bands (126, 160, 171, 192 cm^{-1}, *etc.*) which corresponds to the presence of As rich and S(Se) rich molecular fragments. Two intensive and broad bands at 257 and 353 cm^{-1} are the dominant features. Also it can be seen that, as in the case for glasses, the sum of the Raman spectra for of $As_{40}S_{60}$ and $As_{40}Se_{60}$ films taken with above ratio (1/3 and 2/3, respectively) gives good rough approximation for Raman spectra of $As_{40}S_{20}Se_{40}$ films (Fig.2, curve 2). Differences are in the same spectral region as in the case of glasses. Peak at 260 cm^{-1} can be considered as showing increased presence of the Se_n chains and also to the presence of the mixed $AsS(Se)_{3/2}$ pyramidal structural units. It is necessary to note that the band near 495 cm^{-1}, which is well pronounced in the spectra of $As_{40}S_{60}$ films, is absent in the Raman spectrum of as-evaporated $As_{40}S_{20}Se_{40}$ films. This band is connected with the presence of S-S bonds, and its absence can be considered as indication that almost all sulphur is used in pyramidal units, and it gives an additional support for attribution of the band peaking at 260 cm^{-1} to the somewhat increased presence of Se_n mo-

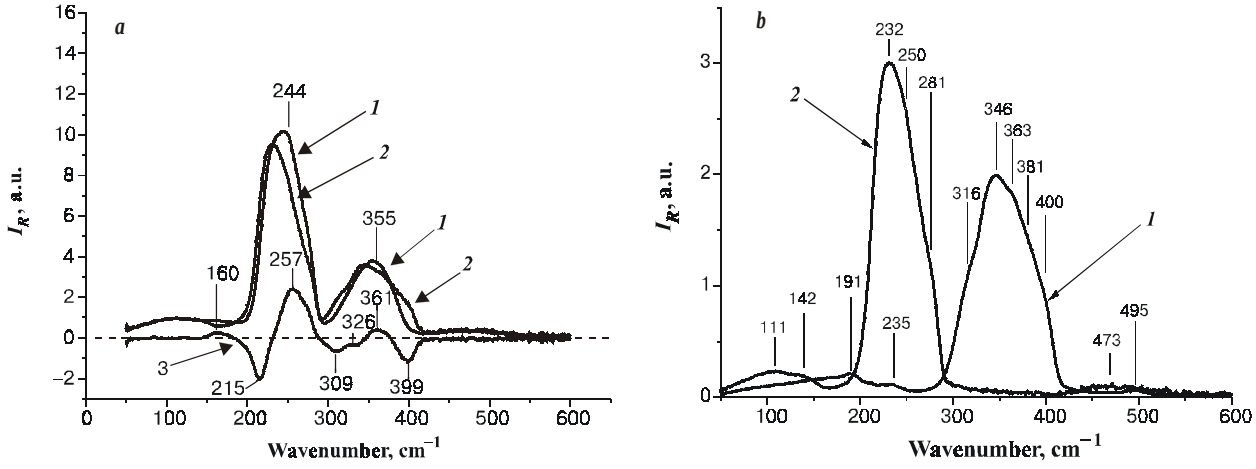

Fig 1. *a* – Raman spectra of $As_{40}S_{20}Se_{40}$ glass – curve *1*. Curve *2* – sum of Raman spectra of $As_{40}Se_{60}$ and $As_{40}S_{60}$ glasses taken in ratio 2/3 and 1/3, respectively. Curve *3* – difference between curves 1 and 2. *b* – Raman spectra of $As_{40}S_{60}$ – curve *1* and $As_{40}Se_{60}$ – curve *2* glasses. Spectra $As_{40}S_{20}Se_{40}$, $As_{40}Se_{60}$ and $As_{40}S_{60}$ glasses were reduced according to Shuker-Gammon procedure and normalized on area.

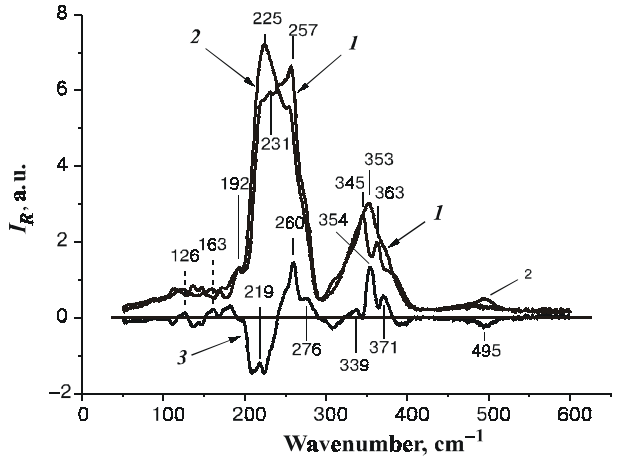

Fig. 2. Raman spectra of as-evaporated $As_{40}S_{20}Se_{40}$ films – curve *1*. Curve *2* – sum of Raman spectra of $As_{40}Se_{60}$ and $As_{40}S_{60}$ films taken in ratio 2/3 and 1/3, respectively. Curve *3* – difference between curves *1* and *2*. Spectra for $As_{40}S_{20}Se_{40}$, $As_{40}Se_{60}$ and $As_{40}S_{60}$ films were reduced according to Shuker-Gammon procedure, normalized on area.

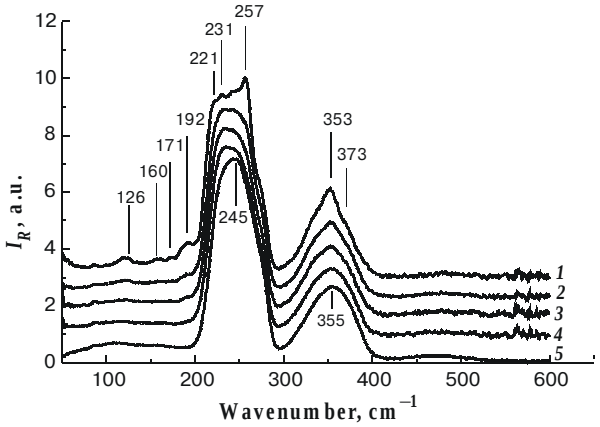

Fig. 3. Raman spectra of $As_{40}S_{20}Se_{40}$: *1* – as-evaporated layers; *2*, *3*, *4* – exposed: halogen lamp (20,40,80 min., respectively); *5* – glass. Spectra were reduced according to Shuker-Gammon procedure, normalized on area and for convenience of observation shifted on equal distance in respect to each other.

lecular fragments. The band in the region 345–380 cm^{-1} with peaks at 354 and 371 cm^{-1} is connected, as in the previously considered case for glasses, with the presence of mixed $AsS(Se)_{3/2}$ pyramidal structural units and As_4S_4 units in addition to $AsS_{3/2}$ and $AsSe_{3/2}$ units in the network of $As_{40}S_{20}Se_{40}$ films. Somewhat increased presence of Se_n and As_4S_4 molecular fragments can be considered as caused by deviation from the statistical behaviour under substitution of Se by S atoms in $As_{40}S_{60-x}Se_x$ glasses [10-12].

As can be seen from Raman spectra (Fig. 3) structure of evaporated $As_{40}S_{20}Se_{40}$ thin films (curve 1) differs from the glass one (curve 5). The structure of the evaporated $As_{40}S_{20}Se_{40}$ film on the basis of the above presented considerations can be presented in the form of matrix, which consists of pyramidal units $AsS_{3/2}$, $AsSe_{3/2}$ and $AsS(Se)_{3/2}$. This matrix also contain considerable amounts of $As_4S(Se)_4$ and $S(Se)_n$ fragments which contain As-As and S(Se)-S(Se) homopolar bonds. Other defects, pores and hollows can be present in the structure as well.

Annealing or exposure results in polymerization of the molecular groups in the main glass matrix, thus the number of homopolar bonds, defects and hollows is decreased. The polymerization process is clearly observed in Raman spectra (Fig. 3, curves 1–4) where with the increase of exposure dose the bands corresponding to the presence of homopolar bonds are decreased in intensity and the spectra became similar to the bulk ones. Photostructural changes start from the initial states, which are determined by the films preparation conditions and are different from the structure of respective glass. Bonds switching under the influence of the external factors (exposure, annealing) with the decrease of the number of homopolar bonds is favourable thermodynamically. Simple consideration of the evolution of the number of homopolar bonds under the exposure gives exponential decay [12]. Photostructural transformations on the microscopic level results in substantial changes in optical, mechanical and chemical properties of the layers. Changes in chemical properties provide possibility to fabricate microreliefs of different types, which can be used in many practical applications.

For example, various holographic protective elements were successfully fabricated using As-S-Se layers.

4. Applicatioon of $As_{40}S_{60-x}Se_x$ layers for fabrication of holographic protective elements

Such inorganic resists are sensitive to visible and ultraviolet radiation and electron beams which enable one to produce master optical-digital holographic elements possessing many safety levels [13]. Samples for investigations were prepared using thermal evaporation of the glass with above mentioned composition in vacuum onto a glass substrate. When exposing photoresist to obtaine interferential 2D/3D patterns, we used electron-beam submicrometer technology and the He-Cd laser radiation with the wavelength $\lambda = 441$ nm [13-14]. The exposure was chosen from the range 20 to 300 mJ/cm^2, and spatial frequencies of obtained gratings were 600 to 1600 mm^{-1}. In addition, resist performances were investigated using the Dot-matrix technology. The resist samples were processed using a waterless organic selective etchant based on amines [15-17]. Topology of obtained microstructures was investigated using atomic force microscope of Nanoscope IIIa Dimension 3000 type.

Results of investigations showed that $As_{40}S_{60-x}Se_x$ (x = 20…40) photoresist is characterized by higher holographic sensitivity (Fig. 4–5). Holographic sensitivity in our case was determined as energetic expose necessary for providing given value of diffraction efficiency. Measurements of diffraction efficiency was carried out using 0.63 mm wavelength.

This enables to get combined optical-digital protective element: digital hologram; optical and digital holo-

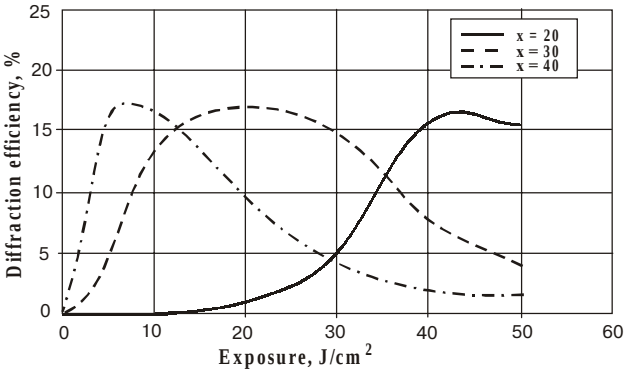

Fig. 4. Holographic sensitivity of $As_{40}S_{60-x}Se_x$ photoresist under recording of diffraction structures by using the wavelength 0.63 μm.

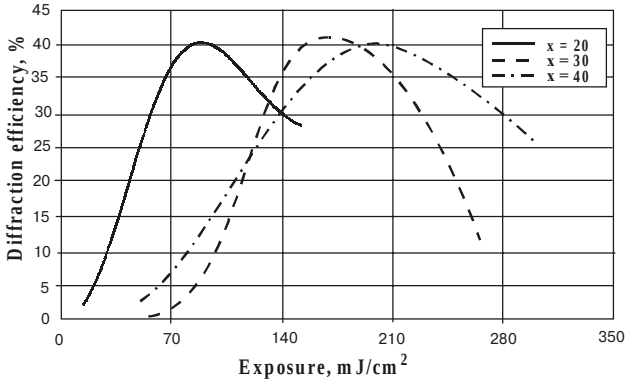

Fig. 5. Holographic sensitivity of $As_{40}S_{60-x}Se_x$ photoresist under recording of diffraction structures by using the wavelength 0.44 μm.

gram; combination of optical and digital hologram with submicrotext image; diffraction structures with heights up to 600 nm and periods down to 950 nm using the Dot-matrix technology.

5. Conclusions

Photostructural transformations in $As_{40}S_{60-x}Se_x$ layers results in polymerization of the molecular groups in the main glass matrix. The number of molecular fragments containing homopolar bonds is decreased as a result of exposure or annealing.

High level of photostructural transformations in $As_{40}S_{60-x}Se_x$ layers provides possibility of their use as recording media in fabrication of holographic protective elements.

Acknowledgments

The authors thank Ministry of Education and Science of Ukraine for financial support and express his gratitude to colleagues from Institute of Semiconductor Physics (NAS of Ukraine), Specialized Enterprizes "Holography" and "Optronics" for their help in carrying out the holographic experiments.

References

1. A.V.Stronski, M.Vlcek, A.Sklenar, P.E.Shepeljavi, S.A.Kostyukevich and T.Wagner, Application of $As_{40}S_{60-X}Se_X$ layers for high-efficiency grating production // *Journ.Non-Cryst.Sol.* **266-269**, I.1-3. p.973-978 (2000).
2. V.Q.Nguen, J.S.Sanghera, I.K.Lloyd, I.D.Aggarwal, D.Gershon, Room temperature dielectric properties of $As_{40}S_{60-X}Se_X$ glass system // *Journ.Non-Cryst.Sol.* **276**, P.151-158 (2000).
3. A.V.Stronski, M.Vlcek, Imaging properties of $As_{40}S_{40}Se_{20}$ layers // *Optoelectronics Review*, **8**, N3, p.63-67 (2000).
4. A.M.Andriesh, M.S.Iovu, S.D.Shutov, Chalcogenide non-crystalline semiconductors in optoelectronics // *Journal of Optoelectronics and Advanced Materials* **4**, N3, p.631-648 (2002).
5. I.D.Aggrawal, J.S Sanghera, Development and applications of chalcogenide glass optical fibers at NRL // *Journal of Optoelectronics and Advanced Materials* **4**, N3, p.665-678 (2002).
6. A.V.Stronski, M.Vlcek, Photosensitive properties of chalcogenide vitreous semiconductors in diffractive and holographic technologies applications// *Journal of Optoelectronics and Advanced Materials* **4**, N3, p.699-704 (2002).
7. R.Shuker, R.Gammon, Raman-scattering selection-rule breaking and the density of states in amorphous materials // *Phys.Rev. Lett.*, **25**, N4, p.222-225, (1970).
8. G.Lucovsky, Optic modes in amorphous As_2S_3 and As_2Se_3 // *Phys.Rev.B*, **6**(4), pp.1480-1489 (1972).
9. I.Fejes, F.Billes, V.Mitsa, A theoretical study of the effect on the vibrational spectrum of the stepwise sulfur by selenium substitution in arsenic pentasulfide // *Journal of Molecular Structure* (Theochem) 531, pp407-414 (2000).
10. A.Feltz, Amorphous Inorganic Materials and Glasses, VCH, Weinheim, 1993, 447p.
11. M.Vlcek, A.V.Stronski, A.Sklenar, T.Wagner, S.O.Kasap, Structure and properties of $As_{40}S_{60-X}Se_X$ glasses // *Journ.Non-Cryst.Sol.* **266-269**, I1-3 p.964-968 (2000).
12. A.V.Stronski, Some peculiarities of the mechanism of irreversible photostructural transformations in thin As-S-Se layers // *Semiconductor Physics, Quantum Electronics & Optoelectronics*, **4** (2), pp.111-117 (2001).
13. Using non-organic resist based on As-S-Se chalcogenide glasses for combined optical/digital security devices, Kostyukevych S.O., Moskalenko N.L., Shepeliavyi P.E., Girnyk V.I., Tverdokhleb I.V., Ivanovsky A.A., Semiconductor Physics, Quantum Electronics & Optoelectronics, 2001, v. 4, # 1, p.70-73.
14. Multilevel computer-generated holograms for reconstructing 3-D images in combined optical-digital security devices, Girnyk V.I., Kostyukevych S.O., Shepeliavyi P.E., Kononov A.V., Borisov I.S., Semiconductor Physics, Quantum Electronics & Optoelectronics, 2002, v. 5, # 1, p. 106-114.
15. Solution for negative etching chalcogenide glasses, Patent on Invention № 2008285, Russian Federation, Indutnyy I.Z., Kostyukevych S.O., Shepeliavyi P.E., priority from 20.06.91, Bulletin 4, 28.02.94.
16. The way of manufacturing holographic diffraction gratings, Patent on Invention № 2165637, Russian Federation, Venger E.F., Kostyukevych S.O., Shepeliavyi P.E., Gol'tsov Yu.G., priority from 17.11.1999, Bulletin 11, 20.04.2001. Declarative Patent on Invention № 36209 A, Ukraine, priority from 17.11.1999, Bulletin 3, 16.04.2001.
17. The way of preparation of negative selective etchant for resist layers of As_2S_3 chalcogenide glass, Patent on Invention № 2165902, Russian Federation, Venger E.F., Kostyukevych S.O., Shepeliavyi P.E., Gol'tsov Yu.G., Borodin Yu.A., Kryuchin A.A., Petrov V.V., priority from 27.07.1999, Bulletin 12, 27.04.2001. Declarative Patent on Invention № 34995 A, Ukraine, priority from 27.07.1999, Bulletin 2, 15.03.2001.